Proceedings

Cosmic Microwave Background Anisotropies

André Cipriano

Faculdade de Ciências da Universidade de Lisboa; andretfcipriano@gmail.com

Received: date; Accepted: date; Published: date

Abstract: The most interesting fact about the Cosmic Microwave Background radiation (CMB) are his temperature anisotropies. They are a huge contribution to revolutionize our understanding of cosmology. In this essay we make an overview relatively to the CMB research and then focus on detail on the various effects that causes temperature fluctuations on the power spectrum.

Keywords: CMB, Cosmic, Background, Background, Radiation, Anisotropies, Temperature, Fluctuations

---

1. CMB Overview

Since its fortuitous discovery in 1965, the Cosmic Microwave Background (CMB) radiation, which was first predicted in 1948 as radiation at 5K at the present time, has become one of the most important observational probes of Big Bang cosmology. This radiation is a relic from the early universe because it directly brings us information from the horizon scale at the epoch of recombination. The spectrum of the CMB is well described by a blackbody function with T = 2.7255 K and could only be realized by the thermal equilibrium between photons, electrons and protons.

Its isotropic nature proves a homogeneous and isotropic universe and it turns out that there are correlated signals beyond the horizon in the angular power spectrum of CMB which can be interpreted as partial evidence for the existence of inflation in the very early universe.

Although several fundamental calculations were done before, it was with the COBE (*Cosmic Background Explorer*) Science Mission detection in 1992 that the interest and activity in this area expanded. The biggest achievement of COBE is the discovery of temperature anisotropies in the CMB sky, the detection of 10^{-5} fluctuations in its temperature.

The study of these anisotropies is the study of the small fluctuations in intensity from point to point across the sky. As we will discuss, these anisotropies provide us with a snapshot of the conditions in the universe about 300000 years after the Big Bang. This snapshot is both our earliest picture of the universe and an encoding of the initial conditions for structure formation.

After COBE's discovery, intensive theoretical work was carried out to understand the nature of CMB temperature anisotropies. From this work, it became more and more clear that a precise measurement of CMB temperature anisotropies with much better angular resolution and higher sensitivity than COBE would lead to a new era of cosmology. The MAP satellite was launched in 2001 and the first results were announced in 2003. Just before the announcement, the mission was renamed to WMAP. The Planck satellite was launched in 2009 together with the Herschel Space Observatory. With more channels at higher frequencies and much better angular resolutions and sensitivities than WMAP, Planck successfully obtained an all sky CMB map and the operation stopped in 2013. The Planck team submitted the first series of results in 2013, and continued to analyzing the rest of the data until now.

Due to this observational front, the field of CMB anisotropies has dramatically advanced. The observations have turned some of our boldest speculations about our Universe into a working cosmological model: namely, that the Universe is spatially flat, consists mainly of dark matter and dark energy, with the small amount of ordinary matter necessary to explain the light element abundances, and all the rich structure in it formed through gravitational instability from quantum mechanical fluctuations when the Universe was a fraction of a second old.

Future observations should pin down certain key cosmological parameters with unprecedented accuracy. These determinations will have profound implications for astrophysics, as well as other disciplines. Particle physicists, for example, will be able to study neutrino masses, theories of inflation impossible to test at accelerators, and the dark energy or cosmological constant.

The most important fact about CMB anisotropies is that the photon distribution is very uniform, perturbations are small, and linear response theory applies. Since they are linear, predictions can be made as precisely as their sources

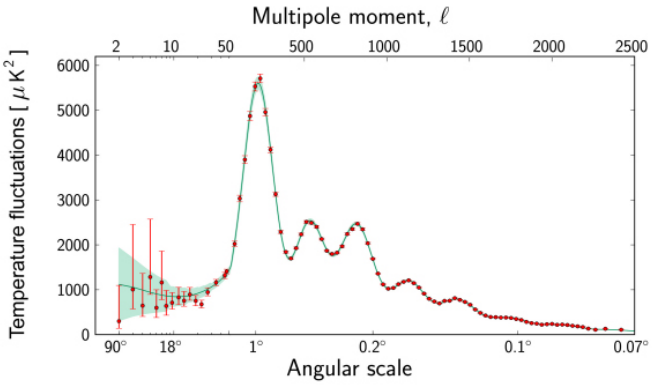

Figure 1. Power spectrum in the Cosmic Microwave Background as seen by Planck. The red dots with error bars are the data points and the green line is the best fit theoretical model. The shaded region indicates the theoretical error from cosmic variance. The precision is essentially cosmic variance limited out to $l \simeq 2000$.

are specified. If the sources of the anisotropies are also linear fluctuations, anisotropy formation falls in the domain of linear perturbation theory. There are then essentially no phenomenological parameters that need to be introduced to account for non-linearities or gas dynamics or any other of a host of astrophysical processes that typically afflict cosmological observations.

Theory predicts, and now observations confirm, that the temperature power spectrum has a series of peaks and troughs. We will talk about the power spectrum origin of these acoustic peaks. Although they are the most prominent features in the spectrum, and are the focus of the current generation of experiments, future observations will turn to even finer details, potentially revealing the physics at the two opposite ends of time.

2. Angular Power Spectrum

The temperature anisotropies of the CMB are described by a 2 dimensional random field. The temperature anisotropies can be expanded in terms of multipole (l) components as:

$$\Delta T/T \equiv \sum_{l=1}^{\infty} \sum_{m=-l}^{l} a_{l_m} Y_{l_m}. \tag{1}$$

where the a_{l_m}, are the multipole moments. In this expansion, low l's correspond to anisotropies on large angular scales while large l's reflect the anisotropies at small scales. The a_{lm} coefficients are independent random variables of mean $< a_{lm} >= 0$. If the temperature fluctuations are statistically isotropic, the variance of the a_{lm} coefficients is independent of m:

$$< a_{lm} a^*_{l'm'} > \equiv C \delta_{ll'} \delta_{mm'} \tag{2}$$

The angular power spectrum C_l is defined by the ensemble average. Accordingly, the ensemble average of square temperature fluctuations is written as:

$$< |\Delta T/T|^2 >= \sum_{ll'mm'} < a_{lm} a^*_{l'm'} m > \int dcos\theta \int d\phi Y_{lm}(\theta,\phi) Y^*_{lm}(\theta,\phi) = \sum_{l}^{\infty} \frac{2l+1}{4\pi} C_l \tag{3}$$

Note here a corresponding angular scale θ for a given l is θ [degree] = $180/l$. From Equation 3, the amplitude of temperature fluctuations in logarithmic space can be described as $l(2l+1)C_l/4\pi$.

The angular power spectrum is shown in Figure 1.

3. Sources of CMB Fluctuations

We will first give a brief summary of all the main effects, and afterwards focus on a more detailed discussion of the specific anisotropies and their dependence on cosmological parameters in the following sections. There are many different ways in which we may choose to categorize the various physical processes that affect the temperature distribution we measure in the microwave sky. We can separate the temperature fluctuations of the CMB into three parts based on individual physical processes as follows:

The primary anisotropies are the temperature fluctuations that were provoked by the processes that occurred until or during the matter radiation period. They divide themselves in the ones that happen due to gravity, Doppler and density fluctuations, in which we can include the main Sachs-Wolfe effect and the acoustic oscilations. Besides that we have the diffusion damping. There are also the topological defects, but this fluctuations are unrelated with the standard model of cosmology.

The secondary anisotropies are generated posteriorly by events that change the background radiation spectrum, as the radiation propagates from the last scattering surface (LSS) until arrives us. They are divided in the ones that happen due to the gravity such as the secondary Sachs-Wolfe effects (the initial Sachs-Wolfe integrated effect and the late Sachs-Wolfe integrated effect), the Rees-Sciama effect and the gravitational lensing. Furthermore we have the effects related to the global reionization such as the suppression, the new Doppler effect and the Vishniac effect. There are also the effects related to the local reionization such as the Sunyaev Zel'dovich (SZ) thermal and cinetic effects.

Besides the primary and secondary anisotropies we also have another effects that contaminate the CMB anisotropy spectrum. These contamination sources are also denominated the tertiary anisotropies. They can be extragalactic, such as radio point and infrared point sources, they can be galactic, such as dust, bremsstrahlung emission or synchrotron radiation, or they can be local, such as the solar system, the atmosphere, noise, etc.

4. Primary Anisotropies

Deviations from the homogeneous and isotropic universe originate from tiny curvature fluctuations generated at the epoch of inflation. Because of their quantum origin in near de Sitter space, curvature fluctuations are expected to have little scale dependence. From the almost scale-free fluctuations, structures of the universe such as galaxies, galaxy clusters, and large-scale structure, as well as CMB temperature fluctuations, are formed. Therefore, any specific structures in CMB temperature anisotropies are generated through physical processes working on the CMB in the expanding universe. The CMB photons that we observe today interacted for the last time with matter for a redshift of approximately 1000, when the universe had about 300000 years of age and when they were at a distance of approximately $6000h^{-1}$ Mpc. With them they transport different finger prints of the region where they suffered the last scattering. Those fingerprints can be modeled by the local potential (ϕ), the peculiar radial velocity of the matter (v_r) and the density fluctuation of the fluid (δ).

Photons that suffered the last scattering in a potential well ($\phi < 0$) experience a gravitational redshift as they move up in that well. Matter dispersed photons by which peculiar velocity is getting away from us ($v_r > 0$), suffer redshift. Photons that come out of a over-density region ($\delta > 0$) have higher temperatures, because denser regions are intrinsically hotter. These three effects can be equated as follows:

$$\frac{\Delta T}{T}(\hat{r}) = \phi(\vec{r}) - \hat{r}.\vec{v}(\vec{r}) + \frac{1}{3}\delta\vec{r} \tag{4}$$

Where $\vec{r}$ is the main distance to the surface of the last scattering, $\hat{r}$ is the versor in the direction $\vec{r}$ and the fields ϕ, $\vec{v}$ and δ must be calculated in the instant of recombination.

4.1. Sachs-Wolfe effect

The first process is gravitational red and/or blue shifts, and was pointed out by Sachs and Wolfe in 1967. The Sachs–Wolfe effect is a simple redshift of CMB photons due to the density fluctuations at the last scattering surface (LSS), which happened at the epoch of recombination when the universe was 3000 K. If there is a higher-density region than the average at LSS, photons from this location have to climb up the potential well ($\phi < 0$) and are gravitationally redshifted.

On the super-horizon scale in the time of recombination, $v >> 1.7^o\Omega_0^{1/2}$, curvature and gravitational potential perturbations (ϕ, $\vec{v}$ and δ) are frozen and keep their initial values as generated in the epoch of inflation. Once the perturbations enter the horizon, curvature and gravitational potential perturbations are damped away in the radiation-dominated epoch, since density perturbations of radiation cannot grow in the sub-horizon scale, although they are preserved in the matter-dominated epoch. Accordingly, the Sachs–Wolfe effect suffers damping on the scales below the horizon of the matter–radiation equality epoch, which is relatively close to the recombination epoch.

It is known that the amount of redshift in the case of adiabatic initial conditions is $\phi/3$, where the initial conditions make coincide the over-density places with the potential wells. On the contrary, the third term in Equation 4 is approximately given by $\delta \approx 2\phi$ for isocurvature initial conditions, and partially cancels with the first term of the second member, resulting in:

$$\Delta T/T(\hat{r}) = \frac{1}{3}\phi(\vec{r}) - \hat{r}.\vec{v}(\vec{r}) \tag{5}$$

The perturbation to the gravitational potential, $\delta\phi$, evaluated on the last scattering surface (LSS), is:

$$\delta T/T = (1/5)R(x_{LSS}) \simeq (1/3)\delta\phi/c^2 \tag{6}$$

This is a result of the combination of gravitational redshift and intrinsic temperature fluctuations.

Since the acoustic oscillations, that we will discuss in the next subsection, provide dominant contributions to temperature anisotropies on the scales below the horizon at the recombination epoch, we can only see the Sachs–Wolfe effect as a dominant contribution in CMB anisotropies on the super-horizon scale at LSS. The horizon scale is defined as $d_H = a\int dt/a$, where $a = 1/(1+z)$ is a scale factor. Accordingly, the comoving horizon scale in the matter-dominated epoch can be written in terms of cosmological parameters as:

$$d_H^c \equiv (1+z)d_H = \frac{2c}{H_0\sqrt{\Omega_M}}(1+z)^{-1/2} \tag{7}$$

where H_0 and Ω_M are the Hubble constant and the matter density parameter at present. Therefore, horizon scales at recombination $1 + z_{rec} \simeq 1100$ and at present are:

$$d_H^c(t_{rec}) = 180(\Omega_M h^2)^{-1/2} Mpc, \tag{8}$$

and,

$$d_H^c(t_0) = 6000(\Omega_M h^2)^{-1/2} Mpc, \tag{9}$$

respectively, in the case of the matter-dominated universe. It should be noted that in the case of the standard flat Λ cold dark matter model, the horizon size at present is 14 Gpc with $\Omega_M = 0.3$ and $h = 0.7$, while Equation 9 gives 16 Gpc, which is 10% larger.

From above equations, we can estimate an angular size of the horizon scale at recombination as

$$\theta_H = d_H^c(t_{rec})/d_H(t_0) = 0.030[radian] = 1.7[degree]. \tag{10}$$

Consequently, we can assume that the Sachs–Wolfe effect provides a dominant contribution on scales larger than 2^o.

The horizon scale (or more precisely, the angle subtended by the Hubble radius) at last scattering corresponds to $l \simeq 100$. Anisotropies at larger scales have not evolved significantly, and consequently directly reflect the "initial conditions".

Assuming that a nearly scale-invariant spectrum of curvature and corresponding density perturbations was laid down at early times (specifically $n \simeq 1$, meaning equal power per decade in k), then $l(l+1)C_l \simeq$ constant at low l_s. This effect is hard to see unless the multipole axis is plotted logarithmically.

4.2. Acoustic Oscillations

For angular scales inferior to sound horizon in the last scattering surface, $v \ll 1.7^o\Omega_0^{1/2}$ $(100 \leq l \leq 1000)$, the fluctuations in ϕ, $\vec{v}$ and δ had time to enter in acoustic oscillations before the initiation of the recombination. This gives origin to Doppler peaks. The position of this peaks is essentially determined by the geometry of the universe, because the same physical scale implies different angular scales for universes with different curvatures. According with:

$$\theta_H \simeq \frac{180}{\pi}\sqrt{\frac{\Omega_0}{z}}[degree] \tag{11}$$

the implied angle by a given scale diminishes with Ω. Consequently, the Doppler peaks move in the direction of the small angular scales (elevated l's) as Ω_0 decreases.

Since photons, protons, and electrons are coupled through Compton and Coulomb interactions before recombination, they can be treated as a mixed compressible fluid. It is known that the density fluctuations in a compressible fluid are acoustic waves. Therefore, perturbations of the mixed fluid start to oscillate once they cross the sound horizon. Here the sound horizon is defined as:

$$d_s \equiv a\int \frac{c_s dt}{a} \tag{12}$$

where c_s is the sound speed. In the case of the photon–baryon mixed fluid, the sound speed can be written as:

$$c_s^2 \equiv \frac{\delta p}{\delta\rho} = \frac{\delta p_\gamma}{\delta(\rho_\gamma+\rho_B)} = \frac{\dot{p_\gamma}}{\dot{\rho_\gamma}+\dot{\rho_B}} = \frac{\frac{4}{3}c^2\rho_\gamma}{4\rho_\gamma+3\rho_B} = \frac{c^2}{3}\frac{1}{1+3\rho_B/4\rho_\gamma} \tag{13}$$

where p is pressure, ρ is density, and suffixes γ and B represent photon and baryon components, respectively.

Once perturbations enter the sound horizon, they start to oscillate as acoustic waves which can be described as $\approx C_{adi}\cos kd_s^c + C_{iso}\sin kd_s^c$, where C_{adi} and C_{iso} are constant factors corresponding to adiabatic and isocurvature initial conditions, respectively, k is the comoving wave number and $d_s^c \equiv d_s/a$ is the comoving sound horizon.

In CMB temperature anisotropies, we can only find acoustic oscillations within the angular scale corresponding to the sound horizon size at the last scattering surface, which can be difficult to obtain as follows.

The comoving sound horizon is approximately written by the use of the comoving horizon as $d_s^c \simeq (c_s/c)d_H^c$, which corresponds to the angular scale:

$$\theta_s = d_s^c(t_{rec})/d_H^c(t_0 \simeq (c_s/c)(1+z_{rec})^{-1/2} = 0.014[radian] = 0.80[degree] \tag{14}$$

At LSS, CMB photons with acoustic modes also suffer gravitational redshift/blueshift to escape from gravitational wells. Besides that, decay of gravitational potential turns out to promote the oscillations due to resonance.

4.3. Diffusion Damping

For small scales, $v < 0.1^o\Omega_0^{1/2}(l > 1000)$, the temperature fluctuations begin to fade. This happens because the process of decoupling of the radiation with matter is not immediate and the last scattering surface is not infinitely thin. Indeed, due to the fact that the decoupling period occurs during an interval of redshifts $\Delta z \simeq 100$, the CMB temperature that is observed in a given direction of the sky is actually an weighted average, corresponding to a mixture of photons coming from the nearer and farthest parts of the LSS. This effect is designated as damping effect and deletes or destroys any fluctuations in smaller scales than the thickness of the LSS.

The diffusion scale can be calculated by employing the random walk process as follows. The number of scatterings of photons by electrons per unit time is $cn_e\sigma_T$, where n_e is the number density of electrons and σ_T is cross section of Thomson scattering. Accordingly, the mean free path of a photon becomes $\lambda_f = 1/n_e\sigma_T$. The diffusion scale due to the random walk can be written as $\lambda_d = \sqrt{N}\lambda_f$, where N is the number of scatterings during the age of the universe. Since the travel distance of a photon $N\lambda_f$ is as long as the horizon size of the universe, which is $2c/H$ in the matter-dominated epoch, N is obtained by the relation $N\lambda_f = 2c/H$, which leads to $\lambda_d = \sqrt{N}\lambda_f = \sqrt{2c\lambda_f/H}$. Therefore, the comoving diffusion scale in the matter dominated era can be written as:

$$\lambda_d^c = (1+z)\lambda_d = 1.62 \times 10^4 (\Omega_M h^2)^{-1/4} (\Omega_B h^2)^{-1/2} (1+z)^{-5/4} Mpc \tag{15}$$

It should be noted that the comoving diffusion scale, below which CMB temperature fluctuations are erased, becomes larger as the universe expands. At the epoch of recombination, $1 + z_{rec} = 1100$,

$$\lambda_d^c(t_{rec}) = 2.55(\Omega_M h^2)^{-1/4} (\Omega_B h^2)^{-1/2} Mpc \tag{16}$$

The corresponding angular scale is:

$$\begin{aligned} \theta_d &= \lambda_d^c(t_{rec})/d_H^c(t_0) = 1.9 \times 10^{-3} (\frac{\Omega_M h^2}{0.15})^{1/4} (\frac{\Omega_B h^2}{0.02})^{-1/2} [radian] \\ &= 6.4 (\frac{\Omega_M h^2}{0.15})^{1/4} (\frac{\Omega_B h^2}{0.02})^{-1/2} [arcmin] \end{aligned} \tag{17}$$

In addiction to diffusion damping, other mechanisms of diffusion destroy and erase the signature of the anisotropies in the small scale region. On small scales, a decrease in the fluctuations of the radiation and the barionic matter in the LSS density fluctuations of photons are damped away due to photon diffusion that drag with them baryons of the overdensity regions. As radiation does not interact with non-baryonic dark matter, this effect doesn't affect the density fluctuations of the constituents of this type of matter.

However, there is another diffusion mechanism (free-streaming) of the overdensity regions to the less dense regions, that can decrease density fluctuations of non-interactive particles (as is the case of dark matter components). This mechanism essentially depends of the velocity and the mass of the particles concerned. Cold particles, which velocity is low (as cold dark matter), are practically unaffected. Particles susceptible of suffering free-streaming like hot dark matter) can show strong decreases in the density fluctuations beginning at a certain physical scale. The physical scale from which this effect becomes significant, depends on the mass of the particles. For instance, for neutrinos with mass $m_v \simeq 10$ eV, the corresponding density fluctuations can be strongly suppressed for inferior scales or in the order of the current size of galaxy super clusters (some Mpc h^{-1}).

The fact that the recombination process is not instantaneous, gives a thickness to the last scattering surface. This leads to a damping of the anisotropies at the highest l's, corresponding to smaller scales than subtended by this thickness. We can also think of the photon-baryon fluid as having imperfect coupling, so that there is diffusion between the two components, and hence the amplitudes of the oscillations decrease with time. This was first pointed out by Silk in 1968, and is often called Silk Damping. These effects lead to a damping of the C's, which cuts off the anisotropies at multipoles above about 2000. So, although in principle it is possible to measure to ever smaller scales, this becomes increasingly difficult in practice.

4.4. Topological Defects

Textures, strings, walls and monopoles are among the examples of topological defects that, according to theory, may have been formed by phase transition mechanisms associated with symmetry breaks of the primordial universe. Although there are currently hybrid models of topological defects and inflation, traditionally the topological models are considered as an alternative theory to the inflationary paradigm for generating density disturbances in the primordial universe.

The full calculation of the power spectrum predicted by defects is much harder than the one for inflation, and consequently the progress in this field has been relatively slow. The main difference from the inflationary paradigm is that all perturbations have to be generated causally, which means, they must be within the horizon volume at a given epoch. Therefore, anisotropies on scales above about 2 degrees have to be generated after recombination, and correspond to late-time effects.

Contrary to what happens in standard inflationary models, CMB anisotropies generated by topological defects have a Non-Gaussianity feature. So far, background radiation observations are not indicative of significant escapes to Gaussianity.

5. Secondary Anisotropies

5.1. Gravity Effects

5.1.1. ISW Effects

In theory, any disturbances in the metrics after the last scattering induce secondary anisotropies effects in background radiation. In Figure 2 we have a graphic representation of the different types of secondary anisotropies.

Time variation of the potentials (the time-dependent metric perturbations) leads to an upturn in the C_l's in the lowest several multipoles. So the dominance of the dark energy at low redshift makes the lowest l's rise above the plateau. Since the overall effect is obtained by integrating the variation of gravitational potential $\dot{\phi}$ over the line of sight, this is called the Integrated Sachs-Wolfe effect (or ISW). This effect takes account of the temperature fluctuations caused by the variation of the gravitational potential along the geodesics of the photons. Admitting only scalar disturbances in metrics, its magnitude is given by

$$\frac{\Delta T}{T} = \int \dot{\phi}[\hat{r}(\eta), \eta] \tag{18}$$

where η is time according to $\dot{\phi} = \partial\phi/\partial\eta$ and the integral is done along the photons flight line.

If a photon crosses a potential well with $\dot{\phi} = 0$, the blueshift acquired in fall is compensated with the redshift it suffers, when the potential well rises. If there is any difference of gravitational potential energy between when photons get into and get out of the structure, the blueshift of the descent and the redshift of the ascent are no longer canceled entirely. The difference of energy generates redshift or blueshift on CMB photons. If $\dot{\phi} > 0$ photons obtain energy and there is a residual blueshift. On the opposite case, when $\dot{\phi} < 0$, the photons lose energy and there is a residual redshift.

The ISW effect generically shows up only at the lowest l's in the power spectrum. The ISW effect is especially important because is extremely sensitive to the dark energy: its amount, equation of state and clustering properties. Specific models can also give additional contributions at low l's (like perturbations in the dark energy component itself). Unfortunately, being confined to this low multipoles, the ISW effect suffers severely from the cosmic variance in its detectability. Perhaps more promising is its correlation with other tracers of the gravitational potential.

Potential decay due to residual radiation, whenever the expansion is dominated by a component whose effective density, is smooth on that scale, but due to dark energy or curvature at late times, induces much different changes in the anisotropy spectrum. What makes the dark energy or curvature contributions different from those due to radiation is the longer length of time over which the potentials decay, on order the Hubble time today. Residual radiation produces its effect quickly, so the distance over which photons feel the effect is much smaller than the wavelength of the potential fluctuation.

The ISW projection, even the projection of all secondary, is much different than the primary anisotropies. Since the duration of the potential change is much longer, photons typically travel through many peaks and troughs of the perturbation. This cancellation implies that many modes have virtually no impact on the photon temperature. The only modes which do have an impact are those with wavevectors perpendicular to the line of sight, so that along the line of sight the photon does not pass through crests and troughs.

In case of linear perturbations during the matter-dominated or radiation-dominated eras, it is known that the gravitational potential (ϕ) of the structure remains constant and accordingly there is no integrated Sachs-Wolfe effect.

There are two types of integrated Sachs-Wolfe effect. The first is called early ISW and the other one is named late ISW, since the transitions take place at $z = 24000\Omega_M h^2$, where h is the non-dimensional Hubble constant normalized to 100 km $s^{-1} Mpc^{-1}$, and at $z = (\Omega_\Lambda/\Omega_M)^{1/3} - 1$, where Ω_Λ is the density parameter of dark energy. Each effect provides a dominant contribution on the comoving horizon scale at the transition epoch in the CMB sky. Accordingly, corresponding angular scales are roughly a degree scale and a few tens of degrees scale for the early and the late ISW effects, respectively.

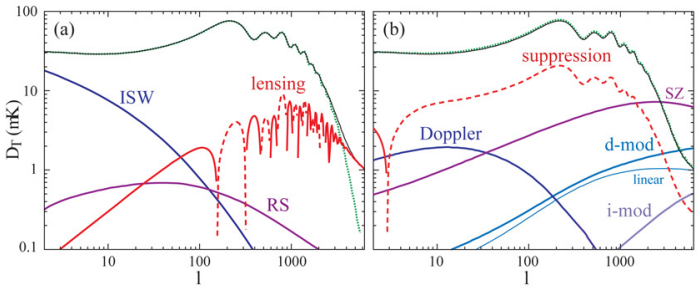

Figure 2. Secondary anosotropies. On the left (a) we have the gravitational secondaries. On the right (b) we have the scattering secondaries.

Early integrated Sachs-Wolfe effect (Early ISW)

For typical models, the period of radiation matter equilibrium occurs just before recombination. Therefore, soon after the last scattering, the radiation density contributes still in a not negligible way to the total density of the universe. As the universe expands and becomes dominated by matter, this causes a decay in the potential ϕ, right after the last scattering, which is called the early ISW effect. Given the fact that the density of the photons is fixed by the current CMB temperature, this effect becomes more important as lower is the total density of the universe, Ω.

In an adiabatic model, radiation pressure makes the potentials decay inside the sound horizon. Consequently the potential fluctuation in a particular wavelength decays as the horizon grows past the wavelength. Wavelengths between the sound horizon at last scattering and at full matter domination can have strongly enhanced anisotropy contributions from this effect. These join smoothly onto driven acoustic contributions and form a potential envelope for the anisotropies.

Late integrated Sachs-Wolfe effect (Late ISW)

In an open or Λ model, the universe experiences sudden changes in the expansion rate, the density fluctuations are frozen in, and the potential (ϕ) again decays for low values of z ($z < \Omega^{-1}$) once expansion is no longer dominated by matter. This leads to a late integrated Sachs-Wolfe effect.

Opposing effects from decaying overdensities and underdensities tend to cancel if the photons can travel across many wavelengths during the decay, as is the case for fluctuations under the horizon size at the end of matter domination.

The projection takes this secondary contributions from the same physical scale to a larger angular scale than the primary Sachs-Wolfe effect because of the intrinsically large size of the horizon at such late epochs and because the point of origin of the effect is much closer than the LSS. The ridgelike structure of the contributions comes from the projection of plane waves onto the sphere. The observable angular power spectrum comes from integrating in k the anisotropy contributions for each multipole.

For a fixed matter density, matter domination ends sooner in an open than a Λ universe. Therefore, the angular scale of the cancellation cut off in the spectrum, is larger in a Λ universe.

5.1.2. Rees-Sciama Effect

The same physical effect caused by non-linear structure formation was first pointed out by Ress and Sciama in 1968 and is denominated the Ress–Sciama effect.

In a linear regime of disturbances, after matter dominance, $\dot{\phi} = 0$. However, as non-linear structures (galaxies and clusters) are formed, the linear regime ceases to be valid and $\dot{\phi}$ ceases to be null. This is an equally "late" effect since the formation of non-linear structures by gravitational collapse, starts only for low redshifts. Although it is still an open issue, everything indicates that the relative intensity of the Rees-Sciama effect is small compared to the amplitude of the primary anisotropies.

Once fluctuations leave the linear regime, their subsequent evolution can also make the potentials vary with time. In hierarchical models, where the smallest scales go non-linear first, this effect peaks toward small scales. In

most reasonable models, the non-linear scale is too small to significantly affect CMB observations above the arcminute regime. Although not likely to be observable by the next generation of experiments, the scale at which fluctuations become nonlinear is in principle also imprinted on the CMB.

5.1.3. Gravitational Lensing

In addition to the ISW effect, gravity can act on background radiation as a gravitational lens.

The gravitational lensing is a complementary effect to the ISW effect, also related to the variation of ϕ along the geodesics of the photons. In the ISW effect, photons loose or gain energy by exchange of small momentum pulses with the gradient of the gravity field parallel to flight line, $\nabla\phi_{\perp}$. However, the perpendicular component to that same line, $\nabla\phi_{\parallel}$, also causes changes in the photons momentum, which in the first order does not change the radiation energy but causes deflections in its trajectory. If θ is the angular distance between two photons without deflections and $\theta + \Delta\theta$ the real angle with deflections, is possible to show that $\Delta\theta/\theta << 1$. For typical models $\Delta\theta/\theta \simeq 0.1 - 0.2$.

This means that this is essentially a weak lensing effect. If we imagine the CMB fluctuations (in the absence of this effect) painted on the surface of a sphere, the lensing action would constitute a stretching and deforming of the sphere, at random. The culminating effect is a distortion of the LSS image. However, as $\Delta\theta/\theta << 1$, these distortions are always injective maps (one-to-one) and therefore in no region the image overlaps over itself.

The final result of this effect is small (typically it introduces variations of less than a few percentage points in the regions of small angular scales) and consists essentially in redistributing power from the peaks to the valleys. Some of the future CMB experiences may detect this effect.

This large coherence and small amplitude ensures that linear theory in the potential is sufficient to describe the main effects of lensing. Since lensing is a one-to-one mapping of the source and image planes, it simply distorts the images formed from the acoustic oscillations in accord with the deflection angle. This warping naturally also distorts the mapping of physical scales in the acoustic peaks to angular scales and consequently smooths features in temperature. The smoothing scale is the coherence scale of the deflection angle $l \approx 60$ and is sufficiently wide to alter the acoustic peaks with $l \approx 300$. The contributions are therefore negative on scales corresponding to the peaks.

Gravitational lensing also generates a small amount of power in the anisotropies on its own but this is only noticeable beyond the damping tail where diffusion has destroyed the primary anisotropies. On these small scales, the anisotropy of the CMB is approximately a pure gradient on the sky and the inhomogeneous distribution of lenses introduces ripples in the gradient on the scale of the lenses.

Because the lensed CMB distribution is not linear in the fluctuations, it is not completely described by changes in the power spectrum. Much work has been done to utilizing the non-Gaussianity to isolate lensing effects and their cross-correlation with the ISW effect. In particular, there is a quadratic combination of the anisotropy data that optimally reconstructs the projected dark matter potentials for use in this cross correlation. The cross correlation is especially important because in a flat universe it is a direct indication of dark energy and can be used to study the properties of the dark energy beyond a simple equation of state.

5.1.4. Gravitational Waves

Gravitational waves can generate secondary anisotropies through the ISW effect. When their action occurs on the radiation spectrum, affects the upper angular scales at the horizon scale at the time of recombination.

This gravitational waves can be viewed as a tensor metric perturbation and produces a quadrupolar distortion in the spatial metric. If its amplitude changes, it leaves a quadrupolar distortion in the CMB temperature distribution. Inflation predicts a nearly scale-invariant spectrum of gravitational waves.

In principle, the mechanism that produces primordial perturbations could generate scalar, vector, and tensor modes. However, the vector (vorticity) modes decay with the expansion of the Universe. The tensors (transverse trace-free perturbations to the metric) generate temperature anisotropies through the integrated effect of the locally anisotropic expansion of space. Since the tensor modes also redshift away after they enter the horizon, they contribute only to angular scales above about 1^o. Consequently some fraction of the low l signal could be due to a gravitational wave contribution, although small amounts of tensors are essentially impossible to discriminate from other effects that might raise the level of the l plateau.

Their amplitude depends strongly on the energy scale of inflation, and its relationship to the curvature fluctuations discriminates between particular models for inflation. Detection of gravitational waves in the CMB therefore provides our best hope to study the particle physics of inflation.

Gravitational waves, like scalar fields, obey the Klein-Gordon equation in a flat universe and their amplitudes begin oscillating and decaying once the perturbation crosses the horizon. While this process occurs even before recombination, rapid Thomson scattering destroys any quadrupole anisotropy that develops. This fact dictates the general structure of the contributions to the power spectrum: they are enhanced at $l = 2$, the present quadrupole, and sharply suppressed at multipole larger than the first peak. As is the case for the ISW effect, confinement to the low multipoles means that the isolation of gravitational waves is severely limited by cosmic variance.

5.2. Reionization and rescattering

If the universe is reionized after the last scattering, free electrons can again disperse the photons from the background cosmic radiation (rescattering). The existence of re-scattering erases the primary anisotropies and creates new anisotropies. This can happen locally, for instance inside a group of galaxies, or globally across the universe.

Inhomogeneous reionization phenomena, caused by stars and quasars formed by elevated redshifts, can also generate (via Doppler effect) secondary anisotropies in background radiation.

5.2.1. Global reionization

Primary anisotropies can be strongly suppressed if the universe has been reionized in a global form for a sufficiently high redshift ($z_r \approx 100$). In the region of small angular scales that suppression can be total. With a global reionization, photons from a given region of the sky do not necessarily have to come from that same direction. Therefore, in a universe where global reonization occurs, the temperature measured in a given sky direction corresponds to a weighted average of temperature of a fraction of the LSS.

The different curves correspond to different z_r redshifts from which the universe suddenly reionized itself and remained so until today. The main conclusions to be drawn are that in the region of large angular scales (small l) the spectrum practically does not change and in the region of small scales (large l) the spectrum is suppressed by a factor $e^{-2\tau}$, where $\tau = \sigma_\tau \int n_e d\eta$ is the optical depth of the universe:

$$\tau \approx \Omega_0^{-1/2} (\frac{h\Omega_B}{0.06})(\frac{z_r}{92})^{3/2} \tag{19}$$

(n_e is the electron density and σ_T is the effective Thomson section).

Vishniac Effect

At very small scales, higher order contributions are more efficient than the Doppler effect in regenerating anisotropies. These generally make use of combining the Doppler effect with variations in the optical depth. For instance, the enhanced baryon density in an overdense region leads to preferential scattering in those regions. If the perturbations are also caught up in a bulk flow, then a Doppler shift arises that can escape cancellation. This is known as the Vishiac effect.

The new temperature fluctuations in the region of small angular scales created by the global reionization originates this effect. Its genesis is related to the coupling of speed fluctuations and free electrons density. It's actually a cinematic effect of the same nature as the kinetic SZ effect that we will talk about in the next segment, related to the linear evolution of density perturbations. The intensity of this effect is small.

5.2.2. Local Reionization

Contrary to what happens with global reionization, it is a given that there are phenomena of local reionization in the universe. The gravitational collapse of gas to the potential wells causes the rising of the particles temperature to the point that they reionize.

For instance, in galaxy clusters, the gas temperature can reach the various tens of millions of degrees Kelvin, a temperature that is clearly enough to keep the hydrogen and helium ionized. The action of local reonization on the

spectrum of the background radiation manifests itself in a characteristic way, through the Sunyaev Zel'dovich effect. This effect is caused by the inverse Compton interaction between the CMB photons and the free electrons of a hot ionised gas along the line of sight, and acts locally at the level of small angular scales. The Sunyaev Zel'dovich effect has an angular power spectrum very similar to Gaussian noise (i.e. C_l constant with l), which is important to "isolate" in order to study separately the information contained in the primary anisotropies of the CMB and in the anisotropies introduced by the SZ effect itself.

Sunyaev Zel'dovich (SZ) effect

Thermal SZ effect The thermal SZ effect is the dominant SZ effect and describes comptonization, the process by which electron scattering brings a photon gas to equilibrium. The term comptonization is used if the electrons are in thermal equilibrium at some temperature T_e, and if both $k_B T_e << m_e c^2$ and $h_{pl}\nu << m_e c^2$, where ν is the frequency of the photon. This defines the non-relativistic nature of the problem. As the electrons are at a higher temperature than the CMB photons, the radiation gains energy, without variation in the number of photons. The spectral distortion of the thermal SZ effect is given by:

$$\Delta I_{th} = I_0 g(x) \int \frac{k_B \sigma_T}{m_e c^2} T_e n_e dl \tag{20}$$

where $I_0 = 2(k_B T_{cmb})^3/(hc)^2$ is a constant, $g(x)$ is a function of dimensionless frequency $x = h\nu/k_B T_{cmb}$ and the integral (done along the line of sight) is the comptonization parameter y. The thermal SZ effect is all the more intense, the higher the density and temperature of the electrons in the direction of the observation line. Its spectral characteristic dependence allows us to separate it from the remaining CMB anisotropies. Experiences, which observed in multiple frequency channels, as in the case of the Planck satellite, already allow seeing a large number (more than a thousand) of thermal SZ sources (galaxy clusters essentially). These observations have great importance, because they allow, in conjunction with X-ray and optical observations, to impose additional constraints in important cosmological parameters such as normalization of the power spectrum of matter e, h and Ω_0. On the other hand, it also makes possible to study the characteristics of matter distribution within the galaxy clusters.

Kinetic SZ effect The SZ kinetic effect happens due to the gas center of mass velocity relatively to the observer referential. If the gas mass is approaching or moving away from the observer, the scattering of CMB photons causes a Doppler effect, which translates into a blueshift or redshift of the photons observed in the direction of the gas mass. The variation of corresponding spectral intensity is given by:

$$\Delta I_k = -I_0 h(x) \frac{v_r}{c} \tau \tag{21}$$

In this expression, $h(x)$ is the function of spectral distortion of the kinetic effect, τ is the optical depth and v_r is the velocity of the center of the gas mass (positive in case of spacing, negative in case of approach) in the observation direction. The kinetic SZ effect is typically weaker than the thermal effect (for typical values of y, v_r and τ the intensity ratio between effects is generally less than 0.1). This fact, associated with an identical spectral dependency to the primary anisotropies, causes the SZ effect kinetics being difficult to observe.

6. Tertiary Anisotropies

They are not CMB anisotropies in the conventional sense. They are rather foregrounds and noises, that overlap, in the same spectral region, to the anisotropies of the cosmic background radiation. In order to have access to the information contained in the primary and secondary CMB anisotropies, it is essential to estimate and remove, in the best possible way, all types of spectral contamination, which may be present in the CMB signal that is observed. Any credible attempt to determine cosmological parameters or information about the primordial universe, which uses background radiation, requires hard work and a profound study of all these contaminations. It is conventional to catalog the various foregrounds as to the proximity of their origin.

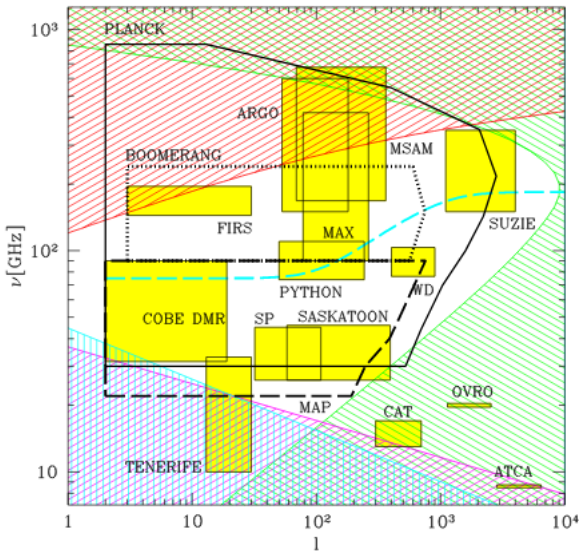

Figure 3. Foregrounds domination. The adopted colours are: light blue - bremsstrahlung, magenta - synchrotron, green - point sources, red - dust. The blue dashed line shows where the total foreground contribution is minimal for each multipole.

Two types of contamination can essentially be distinguished with extra-galactic origin. At low frequencies, ν <300 GHz, contamination is dominated by populations of radio emitting sources. At high frequencies, ν> 300 GHz, emitting sources dominate in the far infrared. Due to the fact of being at great distances, these sources appear as point sources. Its impact on the CMB has a greater expression in the high angular resolution experiences, as is the case of the Planck Mission.

The main sources of CMB contamination are generated in our galaxy. They are dust, bremsstrahlung (free-free) and synchrotron emission. In the first case, interstellar dust grains are heated by visible radiation and re-emit energy in the far infrared. This essentially affects frequencies above ν> 90 GHz (rotating dust grains can also contaminate frequencies between $\approx$ 10 GHz and $\approx$ 100 GHz). The bremsstrahlung emission originates when free electrons interact with the ion potential in the interstellar gas masses, at high temperatures (T> 10^4) , emitting radiation. The frequency range affected is $\nu \approx 25 - 75$ GHz. Finally, the synchrotron emission occurs whenever relativistic electrons are accelerated in magnetic fields, and dominates the remaining galactic contaminations in the region of low frequencies, $\nu < 20$ GHz.

At frequencies around 100 GHz, and for portions of the sky far from the galactic plane, the foregrounds are typically 1 to 10% of the CMB anisotropies. By making observations at multiple frequencies, it is relatively straightforward to separate the various components and determine the CMB signal to the few per cent level. For greater sensitivity, it is necessary to use the spatial information and statistical properties of the foregrounds to separate them from the CMB.

The Foregrounds domination is represented in Figure 3.

There is also local contamination due to the Sun, the Moon, the Earth and other planetary bodies that emit or reflect in the microwave region, and must be taken into account by any experimental device that intends to measure temperature fluctuations of the order of 10^{-5} K. At this temperature scale, the thermal emission of the experimental equipment introduces "electronic" noise in the measurements. Experiences based on land or in balloons, also suffer from the consequences of the atmospheric emission. These are some of the many problems that can affect CMB observations and are naturally treated individually, since they depend directly on experimental equipment characteristics.

7. Bibliography

KOLB, Edward; TURNER, Michael (1990). *The early universe*, Addison Wesley.

PETER, Patrick; UZAN, Jean-Philippe (2009). *Primordial Cosmology*, Oxford University Press.

BOUMANN, Daniel. Cosmology, *Part III Mathematical Tripos*, Course Lectures.

DA SILVA, A. (2012) *Elements of Cosmology and Structure Formation*.

SCOTT, Douglas; SMOOT, George F.(2010). *Cosmic Microwave Background Mini-review*, arXiv:1005.0555.

DURRER, Ruth (2015). *The Cosmic Microwave Background: The history of its experimental investigation and its significance for cosmology*, arXiv:1506.01907.

JONES, A. W.; LASENBY, A. N. (1998). *The Cosmic Microwave Background*, Living Reviews in Relativity.

HU, Wayne; DODELSON, Scott (2002). *Cosmic Microwave Background Anisotropies*, arXiv:astro-ph/0110414.

WHITE, Martin; COHN, J. D. (2002). *TACMB-1: The Theory of Anisotropies in the Cosmic Microwave Background (Bibliographic Resource Letter)*, arXiv:astro-ph/0203120.

SUGIYAMA, Naoshi (2014). *Introduction to temperature anisotropies of Cosmic Microwave Background radiation*, Progress of Theoretical and Experimental Physics.

AGHANIM, Nabila; MAJUMDAR, Subhabrata; SILK, Joseph (2007). *Secondary anisotropies of the CMB*, arXiv:0711.0518.

TEGMARK, Max (1995). *Doppler peaks and all that: CMB anisotropies and what they can tell us*, arXiv:astro-ph/9511148.